Relation between the work function and Young's modulus of RhSi and estimate of Schottky-barrier height at RhSi/Si interface: An ab-initio study

Manish K. Niranjan and Umesh V. Waghmare

Citation: Journal of Applied Physics **112**, 093702 (2012); doi: 10.1063/1.4761994
View online: http://dx.doi.org/10.1063/1.4761994
View Table of Contents: http://scitation.aip.org/content/aip/journal/jap/112/9?ver=pdfcov
Published by the AIP Publishing

Relation between the work function and Young's modulus of RhSi and estimate of Schottky-barrier height at RhSi/Si interface: An *ab-initio* study

Manish K. Niranjan[1,a)] and Umesh V. Waghmare[2]
[1]*Department of Physics; Indian Institute of Technology, Hyderabad, India*
[2]*Theoretical Sciences Unit; Jawaharlal Nehru Center for Advanced Scientific Research, Bangalore, India*

(Received 2 August 2012; accepted 3 October 2012; published online 1 November 2012)

Density-functional calculations are performed to explore the relationship between the work function and Young's modulus of RhSi, and to estimate the *p*-Schottky-barrier height (SBH) at the Si/RhSi(010) interface. It is shown that the Young's modulus and the workfunction of RhSi satisfy the generic sextic relation, proposed recently for elemental metals. The calculated *p*-SBH at the Si/RhSi interface is found to differ only by 0.04 eV in opposite limits, viz., no-pinning and strong pinning. We find that the *p*-SBH is reduced as much as by 0.28 eV due to vacancies at the interface. © *2012 American Institute of Physics*. [http://dx.doi.org/10.1063/1.4761994]

I. INTRODUCTION

Metal silicides are used in silicon based semiconductor devices to form Ohmic contacts and gate electrode due to their low resistance to silicon and excellent compatibility with silicon process technology. In fact they have played an important part in the rapid development of microelectronics.[1–6] In recent years, silicides of platinum and rhodium have been found promising for application as contact materials in nanoscale complementary metal-oxide semiconductor (CMOS) devices due to their low Schottky barrier to *p*-type silicon.[2,7] The silicides of platinum have also been successfully used to develop Schottky-barrier photodiodes (SBD) and detectors. For instance, PtSi/*n*-Si junction based photodiode are used in infrared (IR) imaging system and multiwavelength pyrometry.[8,9] However, these photodiodes carry drawbacks primarily due to suppressed quantum yield by non-radiative photon absorption and increased dark current at increased wavelength.[7] The problems encountered with PtSi/*n*-Si junction based photodiode can be addressed if RhSi is considered in place of PtSi.[7] Besides applications in SBD, the junctions of RhSi with *n*- and *p*-Si have been employed in low power bipolar transistor circuits containing high and low barrier heights.[10] The RhSi is further promising in various nanotechnology applications because of its extremely high corrosion resistance and low cost process.[7,11–16] Although RhSi has been investigated experimentally, very few preliminary theoretical studies of it have been reported. We have recently reported *ab-initio* electronic structure and elastic anisotropy properties of RhSi.[17] In this article, we present an *ab-initio* study of RhSi work functions, Schottky barrier to silicon and their dependence on surface terminations and interface structure respectively, within the framework of density functional theory (DFT).[18] In addition, we also correlate elastic (Young's) modulus with the work function of RhSi and compare the result with a recently reported generic relation for elemental metals.

a)E-mail: manish@iith.ac.in. Tel.: (91)9493595927. Fax: (91)040-23016032.

II. CALCULATION METHODOLOGY

DFT calculations are performed within the Perdew-Burke-Ernzerhoff (PBE)[19] form of generalized gradient approximation as implemented in the VASP package.[20] The electron-ion interactions are approximated by the projected augmented wave (PAW).[2,21] We used a standard plane wave basis set with a kinetic energy cutoff of 350 eV. The surfaces are simulated using supercells in slab geometry of thickness 31.0 Å (10 layers on top of 10 vacuum layers). We use symmetric slabs based on (1×1) surface cells for each termination and keep lateral lattice constant fixed to that derived from the calculated bulk value. The SBH calculations are done by using supercells composed of twenty one layers of (010)-oriented Si on top of thirteen layers of RhSi(010). For the Brillouin zone integration, a $10 \times 1 \times 10$ Monkhorst-Pack mesh is used and each supercell is relaxed until the forces on each atom is reduced to 0.02 eV/Å or less.

III. CRYSTAL AND ELECTRONIC STRUCTURE

Orthorhombic RhSi belongs to *Pnma* space group crystallizing in the MnP-type structure.[22] The primitive unit cell consists four Rh and four Si atoms. The theoretical lattice constants and internal in-plane parameters are within 1-2% of the reported experimental values typical of DFT calculations.[17] As discussed in Ref. 17, the states at the Fermi energy in RhSi are derived primarily from the 4*d* orbitals of Rh atoms. The density of states (DOS) of RhSi at the Fermi level is three times lower than that of bulk Rh, resulting in poor metallic behavior of RhSi. The bonding in RhSi is mixed covalent-metallic type due to hybridization between Rh-4*d* and Si-3*p* orbitals resulting in the formation of three-center (Rh-Si-Rh) directional bonds.[17]

IV. SURFACE ENERGIES AND WORK FUNCTIONS

We calculate work functions and surface energies of stoichiometric and nonstoichiometric (010) surfaces of RhSi. The stoichiometric (010) surface is chosen because of its low surface energy as explained below. The nonstoichiometric surfaces are simulated by creating Rh and Si surface

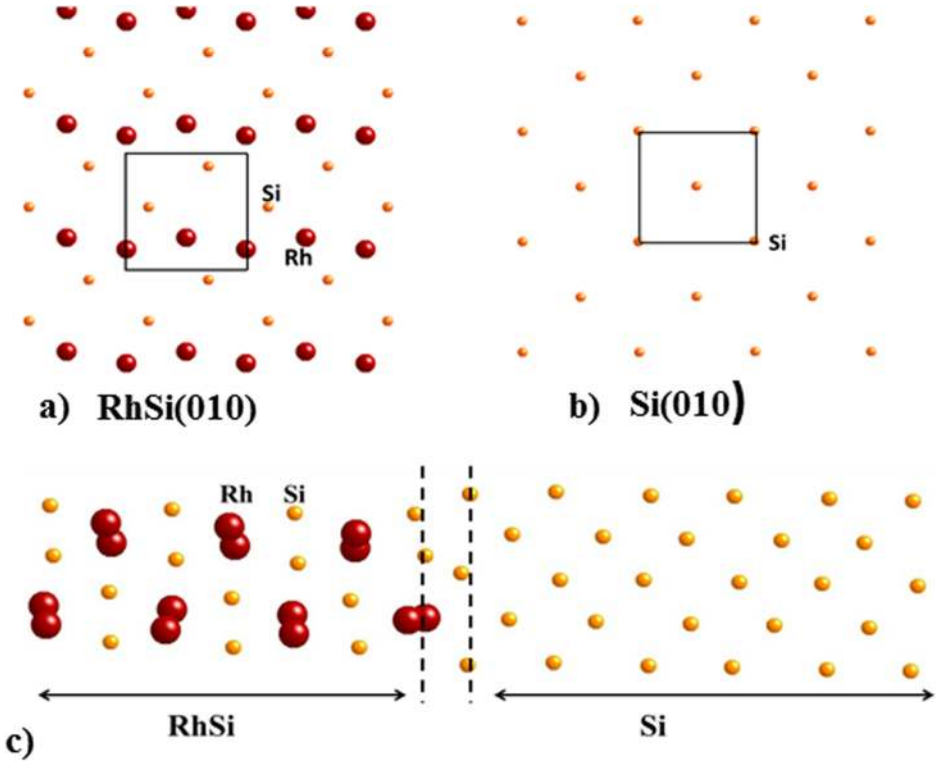

FIG. 1. (a) Top view of the(1×1) surface unit cell of RhSi(010) surface as indicated by bold lines. (b) Top view of the(1×1) surface unit cell of Si (010) surface as indicated by bold lines. (c) Side view of the atomic structure of RhSi/Si(010) supercell.

vacancies. As can be seen in Fig. 1(a), there are two Rh and two Si atoms per surface unit cell. The surface energy of a RhSi surface is estimated using the Gibbs free energy approach[23] and is given by

$$E = \frac{1}{2A}(E_{Slab} - N_{Si}E_{Si} - N_{Rh}E_{Rh} - N_{Si}\mu_{Si} - N_{Rh}\mu_{Rh}). \quad (1)$$

Here, the energy is given per unit surface cell. E_{Slab} is the total energy of the supercell, while E_{Si}, and E_{Rh} are the energies per atom of bulk Si and Rh, respectively. N_{Si} and N_{Rh} are the number of Si and Rh atoms respectively, whereas μ_{Si} and μ_{Rh} are the Si and Rh chemical potential. The introduction of appropriate chemical potentials in the free energy allows us to study the relative stability of surface with different terminations and with surface defects. In equilibrium, the chemical potentials μ_{Si} and μ_{Rh} are related by the condition:

$$\mu_{Si} + \mu_{Rh} = -2(\Delta H_f), \quad (2)$$

where $2(\Delta H_f)$ is the formation energy per formula unit of bulk RhSi. The chemical potentials are measured with respect to their bulk phases ($\mu^{\text{Bulk}} = 0$). Thus, the surface energy can be written as follows:

$$E = \frac{1}{2}\Big(E_{Slab} - N_{Si}E_{Si} - N_{Rh}E_{Rh} + N_{Si}(2\Delta H_f) + \mu_{Rh}(N_{Si} - N_{Rh})\Big). \quad (3)$$

The rhodium chemical potential μ_{Rh} in Eq. (2) is restricted to the energy range bounded by its bulk value ($\mu_{Rh}^{Bulk} = 0$) and RhSi formation energy ($-2\Delta H_f$). In Fig. 2, we show surface energies of stoichiometric (010) surface and that with Rh and Si vacancies as a function of the Rh chemical potential. The zero value of the chemical potential corresponds to Rh rich conditions, beyond that point metallic Rh will start forming on the surface. The range is bounded by the RhSi formation energy, beyond which Si would start forming on the surface. As can be seen from Fig. 2, under Rh-rich condition surface energy of stoichiometric (010) surface is lowest ($\sim$1720 erg/cm^2). The surface energy of this termination remains lowest for μ_{Rh} ranging from 0 to -1.2 eV. However, under Si-rich conditions, the (010) surface with two Rh atoms vacancies, exhibits lowest surface energy. This surface has only two Si atoms per surface unit cell and hence completely Si terminated.

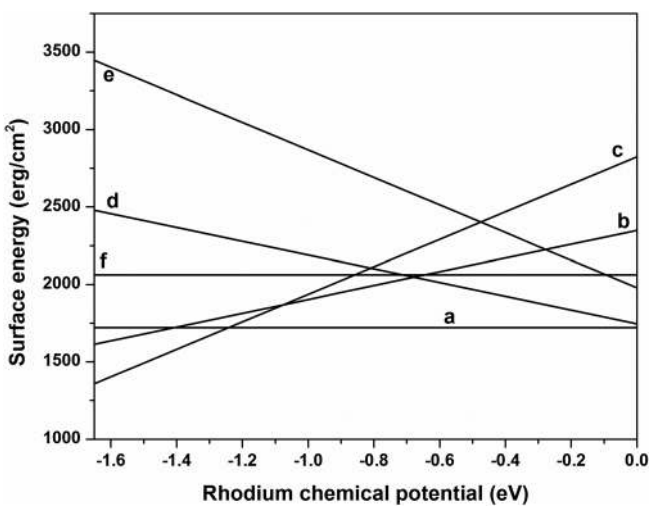

FIG. 2. Surface energies of RhSi(010) surface (a) vacancy-free stoichiometric (0 V), (b) one Rh atom vacancy (1 V_Rh), (c) two Rh atoms vacancy (2 V_Rh), (d) one Si atom vacancy (1 V_Si), (e) two Si atoms (2 V_Si), (f) one Rh-Si pair vacancy (2 V_Rh-Si).

TABLE I. Areal density (ρ_A) of vacancies at RhSi(010) surface, work function (W.F) of RhSi(010) surface with vacancies, and *p*-SBH at Si/RhSi(010) interface with vacancies. Number of vacancies per surface unit cell is indicated by the number preceding the letter "V."

Vacancy	0 V	1 V_Rh	2 V_Rh	1 V_Si	2 V_Si	2 V_Rh-Si
ρ_A (10^{14}/cm^2)	0.0	3.33	6.66	3.33	6.66	6.66
W.F (eV)	4.78	4.58	4.59	4.63	4.32	4.58
p-SBH (eV)	0.41	0.24	0.13	0.40	0.16	0.28

Next, we calculate the work function in slab geometry as $\varphi_m = E_{Vac} - E_{Fermi}$. Here E_{Vac} and E_{Fermi} are the vacuum energy and the Fermi level. The vacuum energy E_{Vac} is estimated by the value of the total electrostatic potential in the vacuum region separating periodic images of the slab. The work function is known to change with the orientation of the metal surface by amounts ranging from 0.1 to 1 eV. The anisotropy is generally attributed to the redistribution of the charge density at the surface, resulting in a different dipole barrier. To assess the accuracy of our calculations, we first calculate the work function of the Rh(001) surface. The calculated value of 5.02 eV is in good agreement with the experimental value of 4.98 eV.[24] Thus we believe the overall accuracy is less a tenth of eV. Table I shows the work functions of various (010) terminations due to vacancies mentioned in the previous section. The work function of clean stoichiometric (010) surface is found to be 4.78 eV and it is lowered by as much as 0.4 eV due to the surface vacancy. The lowest work function value is found for (010) surface with two Si atoms vacancies, although this surface has relatively high surface energy (see Fig. 2). For all other surfaces listed in Table I, the work function is lowered by less than 0.2 eV due to vacancies. The work function for (010) surface with single Rh atom vacancy (has lowest surface energy under Si-rich conditions) is found to be 4.58 eV. The relatively small fluctuation in workfunction indeed shows that RhSi remains promising for device applications.

V. RELATION BETWEEN THE YOUNG'S MODULUS AND WORK FUNCTION

Recently, a generic relation between work function and the Young's modulus of the polycrystalline metal was proposed by Hua *et al.*[25] Here, we test the validity of this relation with our results in case of RhSi. As shown in Ref. 25, the relation between the Young's modulus (E) and the work function (φ) is given as

$$E = \alpha \frac{18 \times 16^6 \pi^{10} \hbar^6 \varepsilon_0{}^9}{e^{16} m^3} \varphi^6 \propto \alpha \varphi^6, \tag{4}$$

where α is the Madelung constant, $\hbar$ is Planck's constant, ε_0 is vacuum permittivity, m is the mass of electron, and e is the elementary charge. The Young's modulus is directly proportional to the product of Madelung constant and the sixth power of the metal work function. The Young's modulus (E) and the work function (φ) of most of the metals satisfy the relation,[25]

$$E_{metal} = a_{metal} \times \phi^6_{metal}, \tag{5}$$

where a_{metal} is 0.02233 and E_{metal} and φ_{metal} are given in GPa and eV, respectively. As reported by us recently,[17] the calculated Young's modulus (E) of RhSi is 254.7 GPa. Taking workfunction for stoichiometric (010) termination as 4.78 eV, the calculated value of a_{RhSi} comes out to be 0.0214, in very good agreement with a_{metal}. It should be noted that generic relation between E and φ of elemental metals as given in Eq. (5) may not be generic in case of metal silicides because of relatively more complex nature of electronic structure and atomic bonding in silicides.

VI. SCHOTTKY BARRIER HEIGHT

Next, we calculate *p*-type Schottky-barrier height (SBH) at the Si/RhSi(010) interface. The *p*-SBH at the metal-semiconductor (M-S) interface is given as the difference between the valence band edge and the Fermi level in the semiconductor band gap. For most metals and semiconductors, the SBH at the M-S interface is known to lie between the no-pinning (Schottky) limit[26] and the strong-pinning (Bardeen) limit.[27] In the no-pinning limit, the SBH varies linearly with the metal work function. On the other hand, in the strong-pinning limit, the SBH does not depend on the metal work function. However, experimentally the SBH shows a weak dependence on the metal work function.[28] This insensitivity of the SBH to the metal work function has often been described as *Fermi level pinning* in the literature.[29] In the no-pinning limit, the *p*-SBH is calculated as the difference between the sum of semiconductor band gap (E_g) and electron affinity (χ), and metal workfunction (φ_m). The calculated values of the work function of RhSi(010) surface and Si electron affinity plus band gap ($\chi + E_g$) are 4.78 eV and 5.10 eV. We estimate $\chi + E_g$ for Si as the difference between vacuum level and top of the valence band of Si(010)-2 × 2 reconstructed surface. With these values, the *p*-type barrier at the RhSi/Si(010) interface is 0.32 eV in the no-pinning limit. In the strong-pinning limit, the Fermi level is assumed to be pinned at the charge neutrality level (ϕ_{CNL}). The charge neutrality level of surface states is defined as the position of the Fermi level which renders the semiconductor surface neutral. At M-S interface, the Fermi level pinning is suggested to be primarily due to metal-induced-gap-states (MIGS).[30] The ϕ_{CNL} in the semiconductor can be identified as the level above which MIGS are empty for a neutral surface[31] and can be calculated as the branch point of the complex band structure of the semiconductor. For the Si, it is calculated to be 0.36 eV above the valence band edge.[31] Thus, in the strong-pinning limit, the *p*-SBH at the Si/RhSi interface would be 0.36 eV. It is remarkable that unlike other metal silicides, the values of *p*-SBH of RhSi in two extreme limits (strong and no-pinning) do not show any significant difference. Nevertheless, a more reasonable estimate of *p*-SBH at the M-S interface can be obtained from the following MIGS model,[28] which basically interpolates between strong-pinning and no-pinning limits in a linear fashion

$$\phi_p = \varphi_{CNL} - S(\varphi_m - \chi - E_g + \varphi_{CNL}). \tag{6}$$

Here, ϕ_{CNL}, ϕ_m, χ, and E_g are the charge neutrality level (above valence band edge), metal work function, electron

affinity and valence band gap of the semiconductor. S is an empirical pinning parameter that describes the screening by the interfacial states and is characteristic of the semiconductor. Empirically S is given by[32]

$$S = \frac{1}{1 + 0.1(\varepsilon_\infty - 1)^2}, \tag{7}$$

where ε_∞ is the high frequency limit of the dielectric constant of the semiconductor. The strong-pinning and no-pinning limits correspond to $S = 0$ and $S = 1$, respectively. With ε_∞ for Si equal to 11.7, the S factor comes out to be 0.08. The electron affinity of Si is 3.97 eV (obtained by adding the measured energy gap to our calculated valence band maximum). From these values, the estimated p-SBH at the Si/RhSi interface comes out to be 0.35 eV, close to the strong-pinning limit. This is expected as the Fermi level at the Si surface is strongly pinned. Experimentally, the p-SBH at Si/RhSi interface is 0.33 eV.[7] The estimates of p-SBH at RhSi/Si in strong and no-pinning limits as well as from MIGS interpolation are in very good agreement with the experimental value. Though useful to obtain quick estimates, there are number of limitations with the semiempirical models, as described in detail in Refs. 29 and 33. Generally, semiempirical models are unable to describe the dependence of the SBH on the interface structure. On the other hand, *ab-initio* calculations properly take into account the interface bonding and, thus, properly describe the dependence of the SBH on the interface atomic structure. We perform first-principles calculations of the p-SBH at Si/RhSi interface by using a supercell composed of twenty one layers of (010)-oriented Si on top of thirteen layers of RhSi(010) in a pseudo-epitaxial arrangement (see Fig. 1(c)). We set the in-plane lattice constants of the Si/RhSi supercell to bulk Si lattice constant value since the assumed substrate is Si and the film grown on it is RhSi. The resulting compressive strain in the RhSi film is accommodated by elongation along the growth direction. The lattice constant b in the direction normal to the interface and all the internal degrees of freedom are optimized by minimizing the energy of the supercell. We consider this calculation as only an estimate due to high strain in RhSi film. For a given structure of the interface, we estimate the overall accuracy of the calculation to be on the order of 0.1 eV. However, we find that the work function of strained RhSi(010) film is increased only by 0.05 eV. Furthermore using Eq. (3), the Si/RhSi(010) interface energy is 2024.7 erg/cm^2. Since the interface energy is not too different from the RhSi surface energy, the bonding at the interface appears quite reasonable, and we expect the estimate of SBH to be relevant. We calculated the SBH at the Si/RhSi interface from the formula:

$$\phi_p = E_F - (\bar{V}_{Si} + E_{VBM}), \tag{8}$$

where the E_F, E_{VBM}, and $\bar{V}_{Si}$ are the Fermi energy, valence band edge position of Si and the macroscopic average potential of Si in Si/RhSi supercell. To obtain these quantities, we first calculate the planar average of the electrostatic potential across the supercell as shown in Fig. 3.[34] The macroscopic

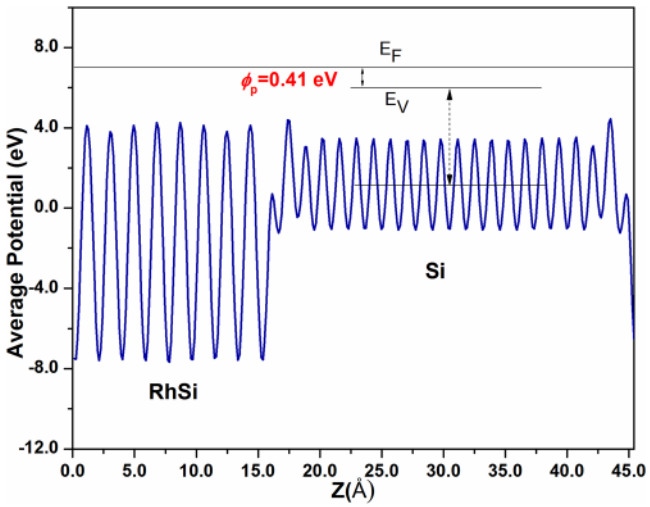

FIG. 3. The average Coulomb potential (in eV) in RhSi/Si(010) supercell along Z (slab axis).

average $\bar{V}_{Si}$ is calculated in the region away from the interface where the character of Si electronic states is bulk-like. From a separate calculation for bulk Si, we find that valence band maximum in bulk Si with respect to macroscopic average potential ($E_{VBM} - \bar{V}_{Si}$) is 5.52 eV. In the supercell, the Fermi energy and the average electrostatic potential in Si region away from the interface are at 7.00 eV and 1.07 eV, respectively. Using the bulk reference to locate the valence band top, we calculate the p-SBH of 0.41 eV from Eq. (8). Our *ab-initio* estimate of p-SBH is in reasonable agreement with MIGS model estimate and the experimental value. The p-SBH can also be inferred from the projected density of states (PDOS) of the Si located in the bulk like region in Si/RhSi(010) supercell. The top of the Si valence band is a triple degenerate p-state at the Gamma (Γ) point. The density of states projected on the p-orbital of Si atom located on layers numbering one to eleven from the interface shows that, into Si region of the supercell farthest from the interface, the valence band maximum is located 0.43 eV below the Fermi energy (see Fig. 4). This gives p-SBH of 0.43 eV

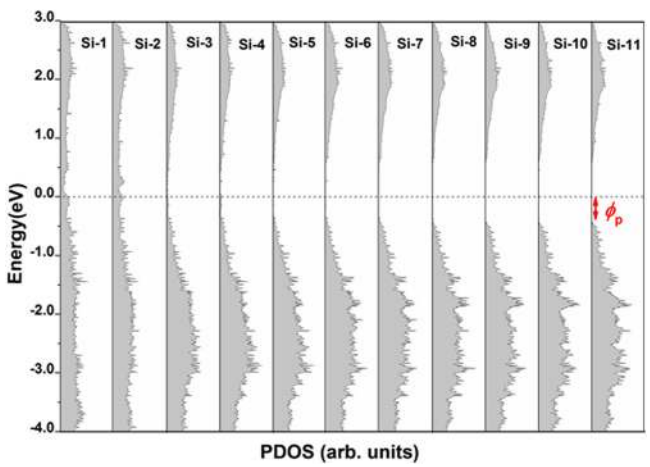

FIG. 4. The partial density of states (PDOS) projected onto p-orbitals of Si atom located on layers in Si region of the RhSi/Si supercell. The number indicates the layer from the interface. The Fermi energy is indicated by the dashed line. φ_p is the p-type Schottky-barrier height.

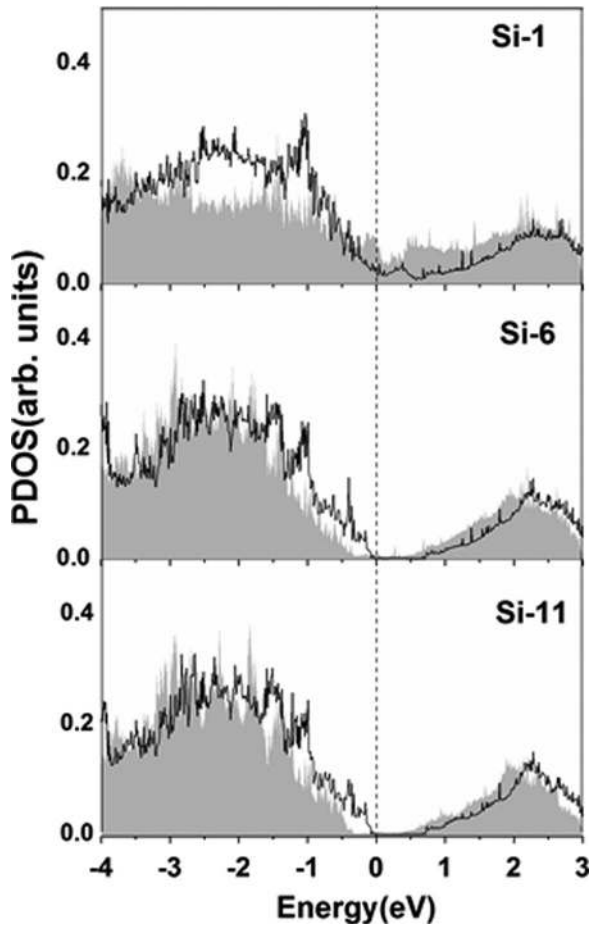

FIG. 5. The PDOS projected onto *p*-orbitals of Si atom located on layers in Si region of the RhSi/Si supercell with two Rh atom vacancies at the interface. The shaded area is the PDOS in the RhSi/Si supercell without interface vacancies (see Fig. 4). The number indicates the layer from the interface. The Fermi energy is indicated by the dashed line.

in close agreement with estimates from the macroscopic potential technique and the MIGS model.

To assess the influence of interface vacancies on the Schottky-barrier, we calculate *p*-SBH at Si/RhSi interfaces with different RhSi(010) surfaces listed in Table I. It can be seen that the Rh or Si vacancies at the interface always tend to lower the *p*-SBH. The *p*-SBH is reduced by approximately 0.17 eV and 0.28 eV due to vacancies created by the removal of one and two Rh atoms, respectively. As seen in Fig. 5, the interface vacancies shifts the Fermi energy towards the valence band edge of Si, thus reducing the *p*-SBH. The *p*-SBH is lowered approximately by 0.01 eV and 0.25 eV due to one and two Si atom interface vacancies respectively. The reduction in *p*-SBH due to single Rh-Si pair vacancy at the interface is ~0.13 eV. These results show that SBH modulation in Si/RhSi can be achieved by creating vacancies at the interface.

VII. CONCLUSIONS

In summary, the calculated Young's modulus and the work function of RhSi are found to satisfy the generic sextic relation between Young's modulus and work functions of elemental metals. The RhSi(010) work function varies by less than 5% due to surface vacancies. The calculated *p*-SBH at the Si/RhSi(010) interface in no-pinning and strong-pinning limits are close to each other and differ by ~8%. The *ab-initio* estimate of *p*-SBH is in reasonable agreement with available experiments. The vacancies at the interface are shown to lower the *p*-SBH value by as much as 0.28 eV. These results are very exciting from scientific as well as application point of view and we hope that our results will stimulate further experiments in this field.

This work was supported by the Department of Science and Technology (DST), Government of India.

[1]S. Zhang and M. Ostling, Crit. Rev. Solid State Mater. Sci. **28**, 1 (2003).
[2]C. Detavernier, A. S. Özcan, J. Jordan-Sweet, E. A. Stach, J. Tersoff, F. M. Ross, and C. Lavoie, Nature (London) **426**, 641 (2003).
[3]*Silicide Technology for Integrated Circuits*, edited by L. J. Chen (IEE, London, 2004).
[4]K. Lu, K. N. Tu, W. W. Wu, L. J. Chen, B. Yoo, and N. V. Myung, Appl. Phys. Lett. **90**, 253111 (2007).
[5]Y. Lin, K. Lu, W. Wu, J. Bai, L. J. Chen, K. N. Tu, and Y. Huang, Nano Lett. **8**(3), 913 (2008).
[6]B. Liu, Y. Wang, S. Dilts, T. S. Mayer, and S. E. Mohney, Nano Lett. **7**(3), 818 (2007).
[7]M. P. Lepselter, A. T. Fiory, and N. M. Ravindra, J. Electron. Mater. **37**(4), 403 (2008).
[8]W. F. Kosonocky, *Review of Schottky-Barrier Imager Technology*, SPIE Advent Technologies Series, Current Overviews in Optical Science and Engineering II, Vol. AT 2, edited By Richard Feinberg (SPIE, 1990), p. 470.
[9]W. F. Kosonocky, M. B. Kaplinsky, N. J. McCaffrey, J. Li, H. Martynov, E. Hou, N. M. Ravindra, C. N. Manikopoulos, S. Belikov, F. M. Tong, and V. Patel, Multi-Wavelength Imaging Pyrometer (M-WIP) for Semiconductor Process Monitoring and Control, Wright Laboratory Final Report for 08/24/92–12/31/94, WI/MTEM WPAFB OH 45433–7739 (US Dept. of Defense, February 1995).
[10]D. A. Hodges, M. P. Lepselter, D. J. Lynes, R. W. MacDonald, A. U. Macrae, and H. A. Waggener, IEEE J. Solid-State Circuits **SC-4**, 280 (1969).
[11]L. Marot, R. Schoch, R. Steiner, V. Thommen, D. Mathys, and E. Meyer, Nanotechnology **21**, 365707 (2010).
[12]E. P. Burte and G. Neuner, Appl. Surf. Sci. **53**, 283–290 (1991).
[13]S. Labich, A. Kohl, E. Taglauer, and H. Knözinger, J. Chem. Phys. **109**, 2052 (1998).
[14]Y. Shapira, P. A. Tove, L. Stolt, and H. Norde, Thin Solid Films **89**(4), 361–366 (1982).
[15]M. E. Schlesinger, J. Phase Equilib. **13**(1), 54–59 (1992).
[16]S. Petersson, E. Mgbenu, and P. A. Tove, Phys. Status Solidi A **36**(1), 217–225 (1976).
[17]M. K. Niranjan, Intermetallics **26**, 150–156 (2012).
[18]W. Kohn and L. J. Sham, Phys. Rev. **140**, A1133 (1965).
[19]J. P. Perdew, K. Burke, and M. Ernzerhoff, Phys. Rev. Lett. **77**, 3865 (1996).
[20]G. Kresse and J. Furthmuller, Phys. Rev. B **54**, 11169 (1996).
[21]P. E. Blöchl, Phys. Rev. B **50**, 17953 (1994).
[22]S. Petersson, R. Anderson, J. Baglin, J. Dempsey, W. Hammer, F. d'Heurle and S. LaPlaca, J. Appl. Phys. **51**(1), 373 (1980).
[23]G. X. Qian, R. M. Martin, and D. J. Chadi, Phys. Rev. B **38**, 7649 (1988).
[24]H. B. Michaelson, J. Appl. Phys. **48**, 4729 (1977).
[25]G. Hua and D. Y. Li, Appl. Phys. Lett. **99**, 041907 (2011).
[26]W. Schottky, Z. Phys. **113**, 367 (1939).
[27]J. Bardeen, Phys. Rev. **71**, 717 (1947).
[28]A. M. Cowley and S. M. Sze, J. Appl. Phys. **36**, 3212 (1965).
[29]R. T. Tung, Mater. Sci. Eng. **R-35**, 1 (2001).
[30]V. Heine, Phys. Rev. **138**, A1689 (1965).
[31]J. Tersoff, Phys. Rev. Lett. **52**, 6, 465 (1984).
[32]W. Monch, Phys. Rev. Lett. **58**, 1260 (1986); W. Monch, Surf. Sci. **299**, 928 (1994).
[33]R. T. Tung, Phys. Rev. Lett. **84**, 6078 (2000).
[34]C. G. Van de Walle and R. M. Martin, Phys. Rev. B **34**, 5621 (1986).